20.5% efficiency on large area N-type PERT cells by ion implantation

Adeline Lanterne, Jerome Le Perchec, Samuel Gall, Marianne Coig, Aurélie Tauzin, Yannick Veschetti

Available online at www.sciencedirect.com

ScienceDirect

Energy Procedia 55 (2014) 437 – 443

Energy Procedia

4th International Conference on Silicon Photovoltaics, SiliconPV 2014

20.5% efficiency on large area N-type PERT cells by ion implantation

Adeline Lanterne[a,*], Jérôme Le Perchec[a], Samuel Gall[a], Marianne Coig[b], Aurélie Tauzin[b], Yannick Veschetti[a]

[a]*CEA, LITEN, INES, 50 av. du Lac Léman, BP332, 73370, Le Bourget du Lac, France*
[b]*CEA, LETI, 17 rue des Martyrs, 38054, Grenoble Cedex 9, France*

Abstract

We developed a high efficiency N-type PERT (Passivated Rear Totally Diffused) bifacial structure based on B and P ion implantation doping, SiO_2 passivation and conventional screen-printing metallization. Two process flows were compared: a "co-anneal" process and a process using separated anneals for B and P activation. We highlight the impact of the variations of the B-emitter and P- BSF profiles on the solar cells performance. The impact of the boron implantation dose was studied allowing to optimize this parameter. Concerning the BSF, two temperature ranges were studied for the P activation leading to very different BSF profiles. A shallower profile enables to reach high implied Voc while keeping low contact resistivity. The overall optimization was integrated into a simplified and industrial process flow on large area Cz-Si solar cells (239cm²). An average efficiency of 19.7% was reached using the "co-annealing" process. The efficiency in this case was limited by a low PFF. This limitation was solved using the "separated anneal" process where an average efficiency of 20.2% was obtained on a 15 cells batch with a 20.5% champion cell.

Peer-review under responsibility of the scientific committee of the SiliconPV 2014 conference

Keywords: n-type silicon; boron; phosphorus; ion implantation; high efficiency; co-annealing

* Corresponding author. Tel.: +33 479 79 20 57;
E-mail address: adeline.lanterne@cea.fr

Peer-review under responsibility of the scientific committee of the SiliconPV 2014 conference
doi:10.1016/j.egypro.2014.08.006

1. Introduction

Although cell manufacturing represents a small part of the global cost of a complete silicon PV system, the choice of the solar cell structure can have a significant impact on the global cost of ownership (CoO). Bifacial solar cells, for instance, have a potential to significantly increase the energy yield in glass/glass modules.

A promising structure for the production of bifacial solar cells is the N-type PERT (Passivated Rear Totally Diffused) process, which has the potential to reach high efficiency while maintaining a cost effective process flow [1]. Indeed N-type silicon solar cells benefit from the advantages of n-type silicon wafers, including the absence of light induced degradation (LID) [2] and a low sensibility to metallic impurities [3]. However the main limitation for the industrialization of N-type PERT solar cells remains the high number of process step due to the formation of two doping regions, a boron doped emitter on the front side and a phosphorus doped BSF (Back Surface Field) on the rear side [4].

Ion implantation has been widely studied these past few years as a potential successor to the standard high temperature gaseous diffusion doping technique [5]. Thanks to its unidirectional doping, it has the advantage of reducing the number of process steps. In the case of N-type PERT solar cells, it allows the process flow to be strongly simplified by removing all the diffusion barrier deposition and removal steps. The best implanted PERT solar cell efficiencies reported so far, using front and rear grids screen-printing metallizations, have already reached 20.5% using Al_2O_3 boron passivation [6]. SiO_2 passivation has also been investigated in several publications but the efficiencies in this case have been limited to 20% due to lower V_{oc} and J_{sc} values [4] [7]. However, Y. Tao in [7] already managed to increase the V_{oc} thanks to a planar rear surface and a lower metal coverage (point contacts).

Compared to Al_2O_3 passivation, SiO_2 brings a significant advantage for industrialization, due to its concomitant growth during the activation annealing, so we focused our study on this latter passivation technique. To solve the V_{oc} and J_{sc} issues observed until now, we studied a large range of B and P profiles using two different process flows: a “co-annealing” process where B and P are activated during the same annealing and a “separated anneals” process where dopants are implanted and activated successively.

2. Experimental

Fig. 1 shows the two process flows investigated in this study. Cz n-type mono-crystal wafers of 3.5 $\Omega.cm^2$ (239 cm^2) were used for the solar cells fabrication. Both processes started by the texturization of the wafers followed by a RCA clean. In the process named “co-anneal”, we performed the B implantation on the front side and the P implantation on the rear side. Both dopants were then co-activated by a thermal anneal at 1050°C. A temperature of 1050°C was used in order to fully activate the boron implanted atoms and to reach a low J_{0e} value [8]. In the “separated anneals” process, the RCA clean was first followed by the B implantation on the front side and its activation at 1050°C. Next, P ions were implanted on the back side and a second activation anneal was applied at a lower temperature range ($T_{max} < 900°C$) .

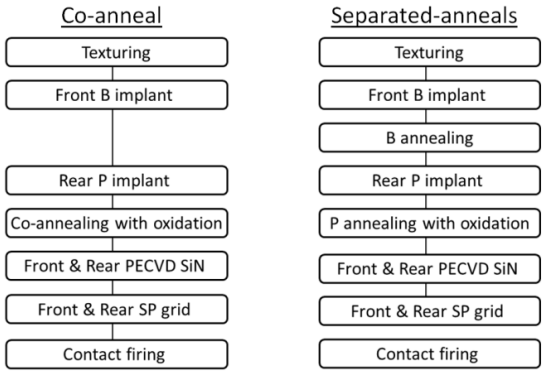

Fig. 1. N-type PERT process flows using ion implantation.

SiO_2/SiN_x passivation stacks were then grown on both surfaces. Contacts were ensured by screen-printing grids of Al/Ag and Ag pastes on the front and rear sides respectively. For the optimization of the implanted emitter and BSF, B and P implantation doses were varied in this study.

Solar cells were characterized by I(V) and Dark I(V) measurements performed on a conductive and reflective back chuck. Contact resistivity on the B- emitter and P- BSF were measured by the method describe by H. H. Berger in [9].

3. Results and discussion

3.1. Boron emitter profile optimization

Fig. 2 (a) shows the SIMS profiles of B implanted emitters resulting from two different implantation doses and activated by an annealing at 1050°C, leading to emitter sheet resistances (R_{sheet}) of 65 Ω/sq and 90 Ω/sq. They are also compared to our standard 65 Ω/sq BCl_3 diffused emitter. For a similar R_{sheet}, the boron implanted emitter profile is less concentrated with a maximum concentration of only 4.10^{19} at/cm^3 when 8.10^{19} at/cm^3 are exceeded in the BCl_3 diffused profile. This concentration decreases further for lower implantation doses with a maximum of 3.10^{19} at/cm^3 in the case of a 90 Ω/sq emitter.

Solar cells were then fabricated using the "separated anneal" process flow for 3 boron implantation doses. It's ended with an emitter sheet resistance ranging from 74 Ω/sq, for the highest implantation dose, to 100 Ω/sq, for the lowest dose. The contact resistivities ($\rho_{contact}$) measured on these emitters are shown on Fig. 2 (b). Despite a slight increase of $\rho_{contact}$ measured for highest R_{sheet}, all values remain below 10 mΩ.cm^2, highlighting a good contact by the Al/Ag paste screen-printed on these low concentrated emitter profiles.

The solar cell parameters, J_{sc} and FF obtained by illuminated I(V) measurements, are shown on Fig. 2 (c) for the 3 different implantation doses. The boron dose reduction is associated with a J_{sc} increase and a simultaneous decrease of the FF. The increase of J_{sc} is well explained by the reduction of the boron concentration in the emitter profiles, which directly improve the blue response. On the other hand, the FF decrease, has been related to the higher R_{sheet} as well as to the slight increase of the front contact resistivity.

Consequently, the best trade-off between J_{sc} and FF corresponded to a 90 Ω/sq B- emitter for our screen-printing conditions.

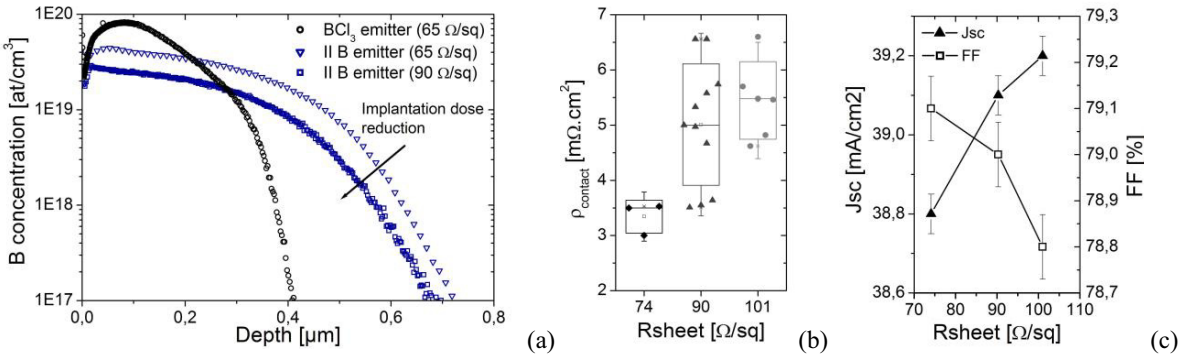

Fig. 2. (a) SIMS profiles of B- emitter implanted at various doses compared to the BCl_3 diffused emitter; (b) front contact resistivity (c) J_{sc} and FF measured on solar cells with various emitter R_{sheet}.

3.2. Phosphorus BSF profile optimization

Contrary to boron, low saturation current densities can be obtained in a P implanted junction with annealing temperatures below 900°C [10]. This allowed us to compare very different P- BSF profiles, using a high annealing temperature in the co-anneal process and a temperature below 900°C in the separated anneals case. Fig. 4 shows the differences observed in the P- BSF profiles for the two annealing temperatures and for various P implantation doses. Profiles were measured by the Electrochemical Capacitance Voltage (ECV) technique. We see that a deeper profile with a lower surface concentration is obtained for the annealing at T=1050°C, whereas the phosphorus concentration decreases for lower P implanted doses for both annealing temperature.

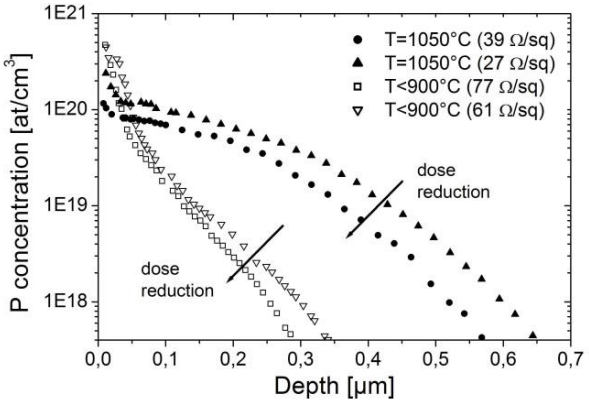

Fig. 3. ECV profiles of P- BSF implanted at various doses and annealed at two different temperatures.

Solar cells were fabricated following each process of Fig. 1 with identical B- emitters of 90 Ω/sq and various P implantation doses. Implied V_{oc} were measured before metallization by the QSSPC technique. Fig. 4 (a) shows a large improvement of the Implied V_{oc} with increasing BSF sheet resistance (or decreasing phosphorus dose), and this for the two BSF annealing temperatures. High implied V_{oc} of 670 mV were reached for both kinds of BSF with the lowest P implantation dose.

Besides, the contact resistivity ($\rho_{contact}$), shown in Fig. 4 (b), was measured on P- implanted BSF formed through annealing at T=1050°C or T<900°C. The $\rho_{contact}$ always increases for a higher R_{sheet}, but was strongly deteriorated for R_{sheet} > 40 Ω/sq in the co-annealing case. Hence, to limit the loss due to contact resistances, the sheet resistance of

the P- BSF was chosen below 40 Ω/sq in the co-anneal process and below 70 Ω/sq for separated anneals.

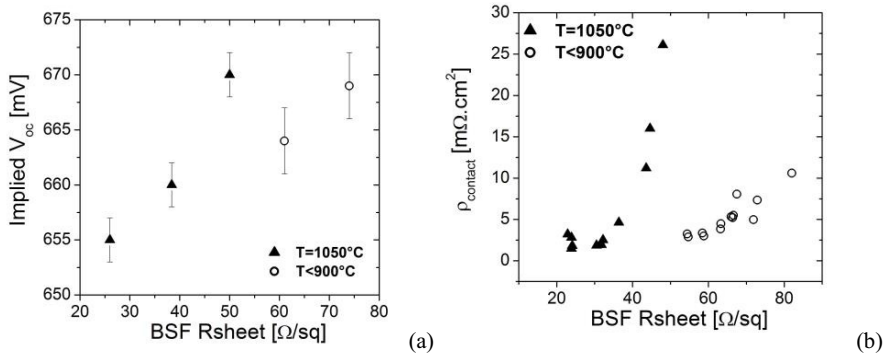

Fig. 4. (a) Implied V_{oc} of implanted PERT solar cells with P- BSF implanted at various doses and annealed at two temperatures, (b) contact resistivity measured on the various BSF.

3.3. N-type PERT implanted solar cells results

Taking into account previous optimizations on the boron emitter and the phosphorus BSF, two batches of 15 cells were fabricated following each process flow (Fig .1), on 239 cm^2 Si-Cz (3-4 Ω.cm) substrates. Table 1 presents the illuminated I(V) results. Both implantation processes led to very high efficiencies: an average efficiency of 20.2% was measured with the separated anneals approach, while 19.7% was measured with the co-anneal process.

Thanks to the implantation dose reductions, the co-anneal process now yields equivalent V_{oc} and J_{sc} values than the separated-anneals-based cells. But the efficiency remains limited by a lower FF. Further characterizations were made to explain the FF difference between both processes. The results of the PFF, measured by SunsVoc, and of the series resistance (R_s) values, calculated by comparing the SunsVoc and the illuminated-IV curves [11], are shown on Table 1. The higher R_s and the lower PFF measured in the co-annealed case both explained the lower FF. The higher R_s was mainly due to a higher $\rho_{contact}$ on the co-annealed BSF, whereas the lower PFF corresponded to a higher J_{02} value of 19 fA/cm^2, when only 2,3 fA/cm^2 was measured in the separated-anneals case. The only difference between both processes is the temperature used for the activation of the implanted P- BSF. It seems that through the J_{02} value, this annealing temperature has a strong impact on the final PFF.

Table 1. Average performances of 15 cells batches.

Cell type	V_{oc} [mV]	J_{sc} [mA.cm^2]	FF [%]	η [%]	PFF [%]	R_s [Ω.cm^2]
Separated anneals	651.5	39.1	79.1	20.2	83.5	0.6
Co-anneal	650.6	39.1	77.3	19.7	82.9	0.75

Table 2 shows the illuminated I(V) parameters of the champion cells obtained with each process since our last optimizations. A maximum efficiency of 20.5% was reached by using the separated-anneals process and 19.9% efficiency by the co-anneal way. They were obtained during separated batches with different optimizations, which explained the gap observed between them in J_{sc} value.

These results were confirmed by the certification of one of the solar cells, similar to the 20.5% cell, which was measured at 20.33% by the Fraunhofer ISE CalLab.

Table 2. Champion cells since last optimizations

Cell typ	V_{oc} [mV]	J_{sc} [mA.cm^2]	FF [%]	η [%]
Separated anneals	652.0	39.4	79.6	20.5
Co-anneal	653.6	39.7	76.8	19.9

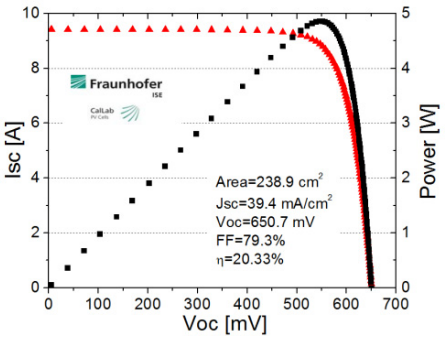

Fig. 5. I(V) performances certified by Fraunhofer ISE of the implanted bifacial PERT solar cells fabricated by the separated anneal process.

4. Conclusion

We succeeded in the development and optimization of a simple and industrialisable process flow for the fabrication of implanted N-type bifacial solar cells. By using two ion implantation steps, a single co-annealing to activate both dopants, and a SiO_2/SiN_x passivation stack, an average efficiency of 19,7% was reached. The annealing temperature used for the activation of the phosphorus has shown a strong influence on the overall FF and PFF. For this reason, by resorting to a lower temperature for the P- BSF activation (separated anneals), a 20.2% average efficiency was obtained, with a champion cell at 20,5%.

With these promising results we are confidant that further optimizations on the screen-printing metallizations should allow to exceed 20% efficiency soon in this co-anneal process as well.

References

[1] R. Kopecek & J. Libal. “The status and future of industrial n-type silicon solar cells” *Photovoltaics International*, 2013.

[2] B. Sopori, P. Basnyat, S. Devayajanam, S. Shet, V. Mehta, J. Binns, and J. Appel, “Understanding light-induced degradation of c-Si solar cells,” *38th IEEE Photovoltaic Specialists Conference,* pp. 1115 - 1120, 2012.

[3] D. Macdonald & L. J. Geerligs, “Recombination activity of interstitial iron and other transition metal point defects in p- and n-type crystalline silicon,” *Applied Physics Letters,* vol. 85, no. 18, pp. 4061-4063, 2004.

[4] S. Gall, A. Lanterne, S. Manuel, V. Sanzone, , R. Cabal, Y. Veschetti, A. Bettinelli, H. Robin, P. Lefillastre, C. Gillot. “High efficient Industrial n-type Technology: From cell to module” *proceeding of the 28th EU PVSEC,* Paris, France, 2013.

[5] A. Rohatgi, D. L. Meier, B. McPherson, Y.-W. Ok, A. D. Upadhyaya, J.-H. Lai, and F. Zimbardi, “*High-throughput ion-implantation for low-cost high-efficiency silicon solar cells*,” Energy Procedia, vol. 15, pp. 10-19, Jan. 2012.

[6] T. S. Böscke, D. Kania, C. Schöllhorn, D. Stichtenoth, A. Helbig, P. Sadler, M. Braun, M. Dupke, M. Weiss, A. Grohe, J. Lossen, and H-J. Krokoszinski “Fully Ion Implanted and Coactivated Industrial n-Type Cells With 20.5% Efficiency” *Proceeding of the 39th IEEE PVSC*, Tampa, Florida, USA, 2013.

[7] Y. Tao, Y-W, Ok, Francesco Zimbardi, A.D. Upadhyaya, J-H Lai, S. Ning, V.D. Upadhyaya and A. Rohatgi. “Fully ion-implanted and screen-printed 20.2% efficient front junction silicon cells on 239cm2 n-type Cz substrate” *Proceeding of the 39th IEEE PVSC,* Tampa, Florida, USA, 2013.

[8] R. Müller, J. Benick, N. Bateman, J. Schön, C. Reichel, A. Richter, M. Hermle, and S. W. Glunz, "Evaluation of implantation annealing for highly-doped selective boron emitters suitable for screen-printed contacts," Solar Energy Materials & Solar Cells, vol. 120, Part A, pp.431-435, Jan. 2014.
[9] H. H. Berger, "Model for contacts to planar devices" *J. Eletrochem. Soc.* Vol. 119 no. 4, pp. 507-514, 1972.
[10] A. Lanterne et al. "Diffused and Implanted Boron Emitter toward High Efficiency N-type PERT Solar Cells" presented to the 3th nPV workshop, Chambery, France, 2013.
[11] D. Pysch, A. Mette, SW Glunz. *Solar Energy Materials & Solar Cells,* vol. 91, pp. 1698–1706, 2007.